The small k_T region in Drell-Yan production at next-to-leading order with the Parton Branching Method

EPS 2023

Sara Taheri Monfared on behalf of the CASCADE group

Introduction: DY p_T spectrum

Why small p_T region in DY?

DY provides a clean, high-resolution final state for better understanding of various QCD effects.

Fred Olness, CTEQ summerschool 2003

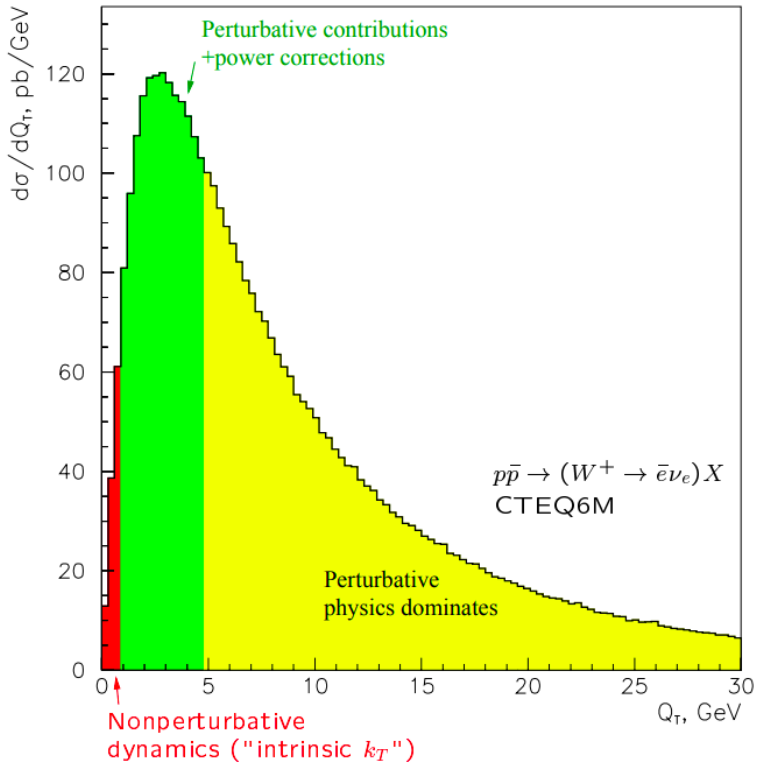

Description of DY p_T spectrum can be divided into three theoretical regions:

- **Perturbative region:** Collinear factrorization theorem suffices to describe the hard real emissions, perturbative higher-order contributions dominant
- **Transition region:** Soft emissions important, no clear separation between perturbative and non-perturbative effects!
- **Non-perturbative region:** Predominantly sensitive to intrinsic k_T and very soft gluon emission

Today's Focus: Exploring intrinsic k_T contribution in PB-set2 via low p_T DY data tuning.
As a first step, we'll explore the potential contributions from various processes in this specific region.

The Parton Branching (PB) method

Evolution for both collinear and TMD PDFs

Parton BR approach provides angular ordered evolution for TMD parton densities
PB-Set1 (with DGLAP-type αs(μ2)) and PB-Set2 (with angular-ordered scale $\alpha_s(p_T^2 = \mu^2(1-z)^2)$):

$$\widetilde{\mathcal{A}}_a(x, k_\perp^2, \mu^2) = \widetilde{\mathcal{A}}_a(x, k_\perp^2, \mu_0^2)\Delta_a(\mu^2, \mu_0^2) + \int \frac{\mathrm{d}^2\mu'_\perp}{\mu'^2_\perp}\Delta_a(\mu^2, \mu'^2_\perp)\Theta(\mu^2 - \mu'^2_\perp)\Theta(\mu'^2_\perp - \mu_0^2) \times \sum_b \int_x^{z_M} \mathrm{d}z P_{ab}^R(z, \alpha_s)\widetilde{\mathcal{A}}_b\left(\frac{x}{z}, (k_\perp + (1-z)\mu'_\perp)^2, \mu'^2_\perp\right) ,$$

z_M : soft gluon resolution parameter
For $z_M \sim 1$: we recover DGLAP

and collinear parton densities:

$$\widetilde{f}_a(x, \mu^2) = \widetilde{f}_a(x, \mu_0^2)\Delta_a(\mu^2, \mu_0^2) + \int_{\mu_0^2}^{\mu^2} \frac{\mathrm{d}\mu'^2}{\mu'^2}\Delta_a(\mu^2, \mu'^2)\sum_b \int_x^{z_M} \mathrm{d}z P_{ab}^R(z, \alpha_s)\widetilde{f}_b\left(\frac{x}{z}, \mu'^2\right)$$

initial distribution is factorized in a collinear part and a normalized Gaussian factor with the width defined by the $\mathbf{q_s}$ parameter

$$\widetilde{\mathcal{A}}_a(x, k_{\perp,0}^2, \mu_0^2) = x f_a(x, \mu_0^2) \cdot \frac{1}{q_s^2} \exp\left(-\frac{k_{\perp,0}^2}{q_s^2}\right)$$

Non-perturbative contribution (I): Non-pert. Sudakov form factor

Factorizing to small and large z region: Perturbative and Non-perturbative sudakov form factor

Sudakov form factors: the probability to evolve from one scale to another scale without resolvable branching
z_{dyn}: an intermadiate scale introduced to divide the two regions with different treatments of the strong coupling

$$\Delta_a(\mu^2, \mu_0^2) \approx \exp\left(- \int_{\mu_0^2}^{\mu^2} \frac{\mathrm{d}\mu'^2}{\mu'^2} \left(\int_0^{z_M} k_a(\alpha_s) \frac{1}{1-z} \mathrm{d}z - d_a(\alpha_s) \right) \right)$$

$$\boxed{z_{\text{dyn}}(\mu') = 1 - q_0/\mu'}$$

$$\Delta_a(\mu^2, \mu_0^2) = \boxed{\exp\left(- \int_{\mu_0^2}^{\mu^2} \frac{d\mu'^2}{\mu'^2} \left[\int_0^{z_{\text{dyn}}(\mu')} dz \frac{k_a(\alpha_s)}{1-z} - d_a(\alpha_s) \right] \right)}$$
$$\boxed{\times \exp\left(- \int_{\mu_0^2}^{\mu^2} \frac{d\mu'^2}{\mu'^2} \int_{z_{\text{dyn}}(\mu')}^{z_M} dz \frac{k_a(\alpha_s)}{1-z} \right)} .$$

Perturbative: $z < z_{dyn} \Leftrightarrow q_\perp > q_0$

$$\Delta_a(\mu^2, \mu_0^2) = \boxed{\Delta_a^{(\mathrm{P})}\left(\mu^2, \mu_0^2, q_0\right)} \cdot \boxed{\Delta_a^{(\mathrm{NP})}\left(\mu^2, \mu_0^2, \epsilon, q_0^2\right)}$$

Non-Perturbative: $z_{dyn} < z < z_M$ (z_M=1-ε)$\Leftrightarrow q_\perp < q_0$
α_s will become large: we freeze α_s at q_{cut}=1 GeV

Motivation for the use of the dynamical resolution scale:
1) To reach the same sudakov form factor of the CSS formalism (Already shown in Alexandra Lelek's talk).
2) To show how the non-perturbative Sudakov affects both the PDF and the TMDs by allowing really soft emissions

Role of soft contributions in PDFs

Limitting z_M leads distributions which are not consistent with the collinear MS factorization scheme

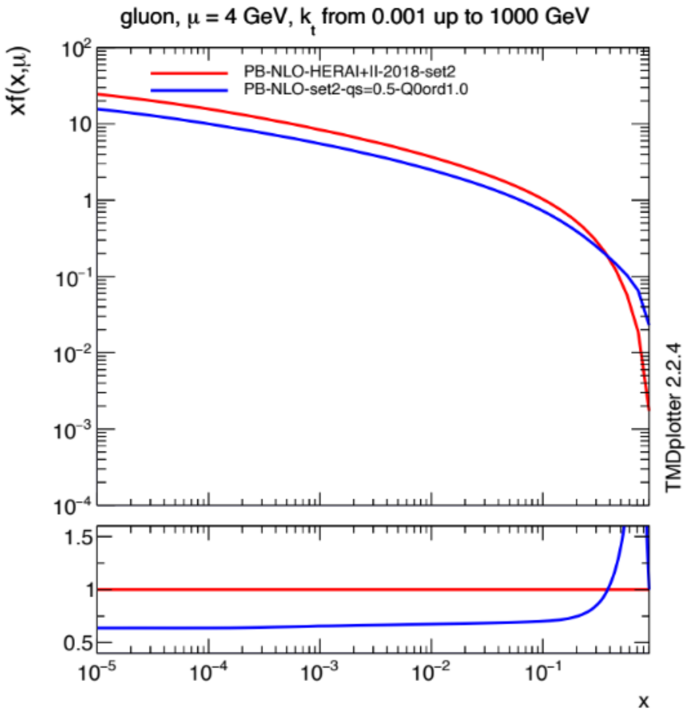

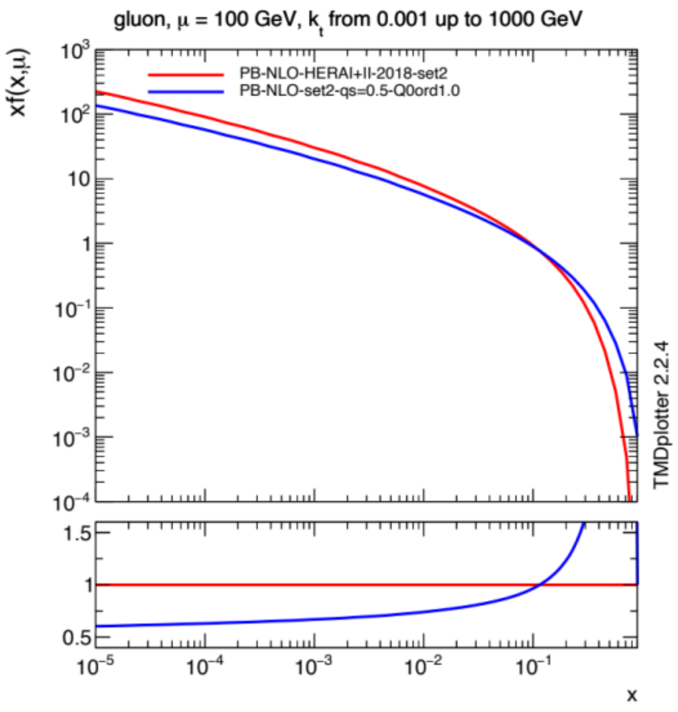

Red: PB-TMD (z_M~1 : Non-pert Sudakov already included)

Blue: PB-TMD with q_0=1.0 GeV (No Non-pert Sudakov)

The distributions obtained from PB-NLO-2018 set2 are significantly different from those applying $z_M = z_{dyn}$, illustrating the importance of soft contributions even for collinear distributions (to have proper cancellation of virtual and real emissions).

Role of soft contributions in TMDs

The effect of the z_M cutoff is even more visible in TMDs!

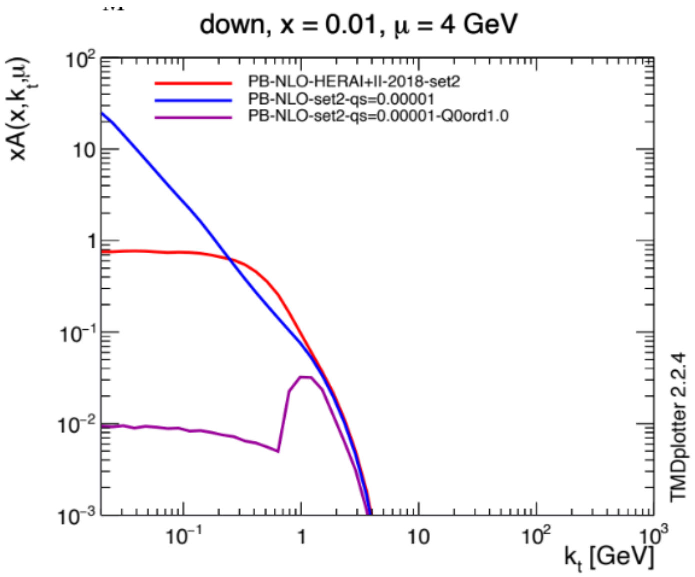

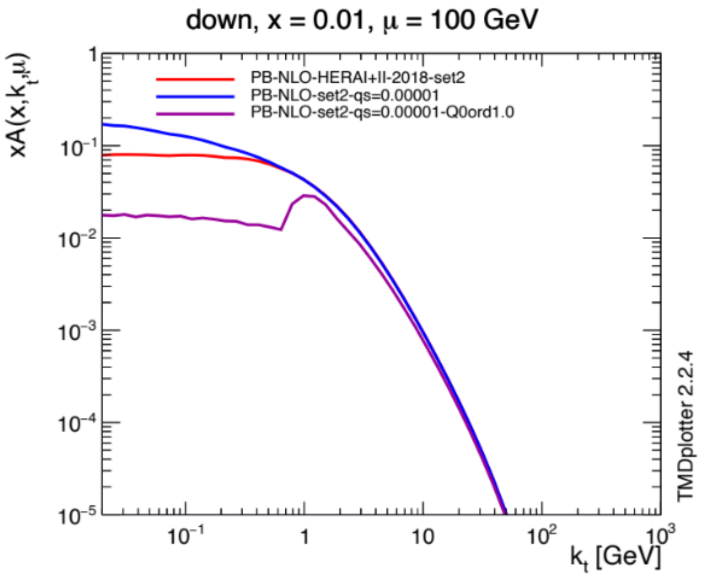

$$z_M = z_{\rm dyn} = 1 - q_0/\mu'$$

Red: PB-TMD, q_s=0.5 (z_M~1: Non-pert Sudakov)

- The non-pert sudakov allows the radiation of very soft gluons with $z_M \to 1$
- Special treatment of α_s is required

Blue: PB-TMD, q_s=0.0 (z_M~1: Non-pert Sudakov + No intrinsic k_t)

- Effect of the intrinsic k_T distribution is much reduced at large scales

Purple: PB-TMD with q_0=1 GeV, q_s=0 (No Non-pert Sudakov + No intrinsic k_t)

- $k_T > q_0$ is not affected by the choice of z_M , while the soft region is significantly affected
- Emissions below q_0=1 GeV are not allowed: There are contributions coming from adding vectorially all intermediate emissions

Non-perturbative contribution (II): Non-pert. distribution

Intrinsic k_T

Transverse momenta of partons in colliding hadrons due to Fermi motion.
Not calculable in perturbative QCD.
Described by phenomenological models
Modelled using a tunable parameter, q_s, through a Gaussian distribution
First assuption was q_s=0.5 GeV

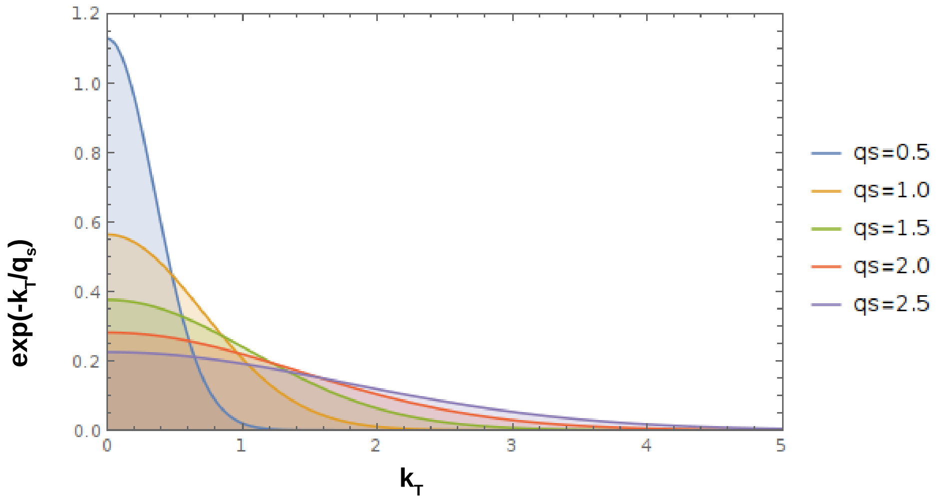

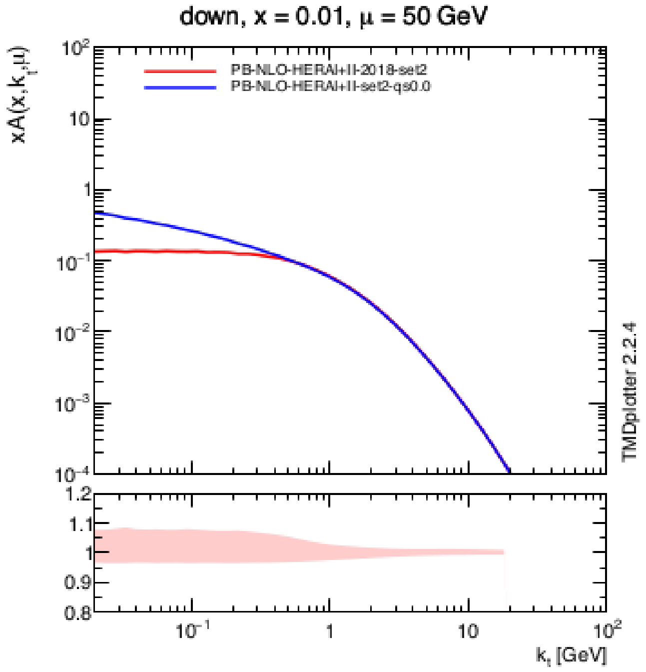

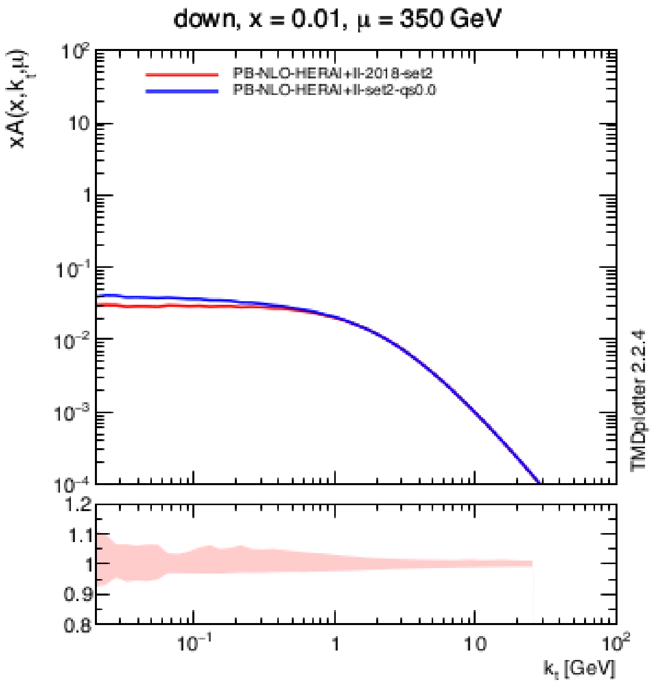

Significant effect of the intrinsic-k_T at low scales

Tuning the Intrinsic k_T parameter

Required settings to calculate the transverse momentum spectrum of DY lepton pairs

Our setting: We use PB-set2 [$\alpha_s(p_T)$] with q_{cut}=1 GeV and $\alpha_s(M_z)$=0.118

Hard process:

- NLO hard-scattering ME are generated by the MADGRAPH_AMC@NLO based on collinear PB-set2
- HERWIG6 subtraction terms are used since they are based on the same angular ordering conditions

Soft process:

- k_T is added to ME by an algorithm in CASCADE using the subtractive matching procedure

Fit of the Gauss width in pp at 13 TeV

How to find the best q_s?

Results obtained from public Eur. Phys. J. C 83 (2023) 628 analysis

- m_{DY}= [50,76], [76,106], [106-170], [170-350], [350-1000] GeV
- Detailed uncertainty breakdown: complete treatement of experimental uncertainties + correlations between bins of the measurement
- Variable: $p_T(ll)$ – analysing up to the peak in the p_T range to maximize the sensitivity to intrinsic k_T distribution
- At higher DY transverse momenta, higher order contributions in the matrix element have to be taken into account
- We vary the q_s parameter and calculate a χ^2 to quantify the model agreement to the measurement.

$$\chi^2 = \sum_{i,k} (m_i - \mu_i) C_{ik}^{-1} (m_k - \mu_k),$$

Eur. Phys. J. C 83 (2023) 628

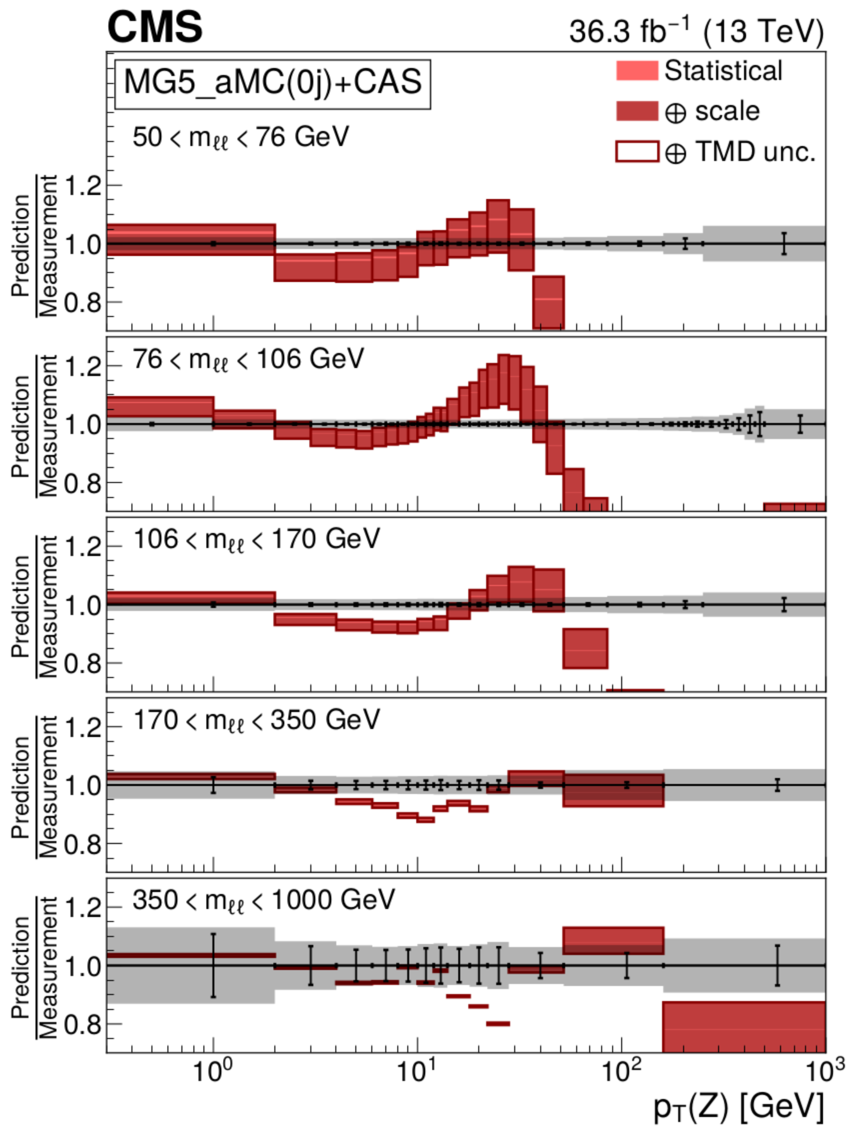

The Gauss width obtained in each m_{DY} bin

The region sensetive to q_s, $p_T(ll)$ < 8 GeV is considered

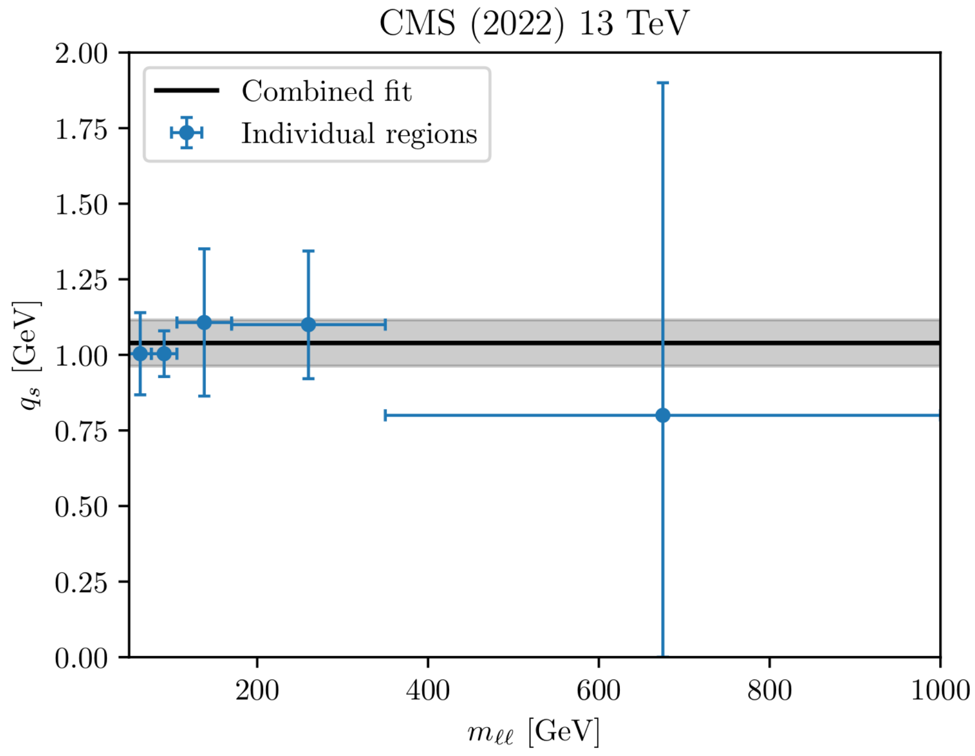

Final q_s extracted from combined covariance matrix analysis across 5 mass bins

- One-sigma confidence obtained as the region of all q_s values for which $\chi^2(q_s) < \chi_{min}^2 + 1$
- Scan resolution and bin uncertainties are taken into account

$\boxed{q_s = 1.04 \pm 0.08 \text{ GeV}}$

Harmonious q_s: The values extracted from all m_{DY} interval are compatible with each other.
Peak Precision: The most precise determination is obtained from the z peak region.
Sensitivity check: The sensitivity at high mass suffers from larger statistical uncertainties in the measurement. Moreover the high mass is less sensitive to q_s

Data used to test the Gauss width at various energies

Global fit of q_s by calculating χ^2 from different measurements

No full error breakdown is available for the other measurements
All uncertainties treated as being uncorrelated and no systematic uncertainty from scale variation in the theoretical calculation
p_T cut:

- **Lower CM energies:** limited $p_T(\ell\ell)$ range → Analyzing intrinsic-k_T impact across entire $p_T(\ell\ell)$ range.
- **Higher CM energies:** Investigating up to peak region

Analysis	$\sqrt{s}$	Collision types	ndf
CMS (2022)	13 TeV	pp	25
LHCb (2022)	13 TeV	pp	5
CMS (2021)	8.1 TeV	pPb	5
ATLAS (2015)	8 TeV	pp	8
CDF (2012)	1.96 TeV	$p\bar{p}$	6
CDF (2000)	1.8 TeV	$p\bar{p}$	5
D0 (2000)	1.8 TeV	$p\bar{p}$	4
PHENIX (2019)	200 GeV	$p\bar{p}$	12
E605 (1991)	38.8 GeV	pp	11
Total			81

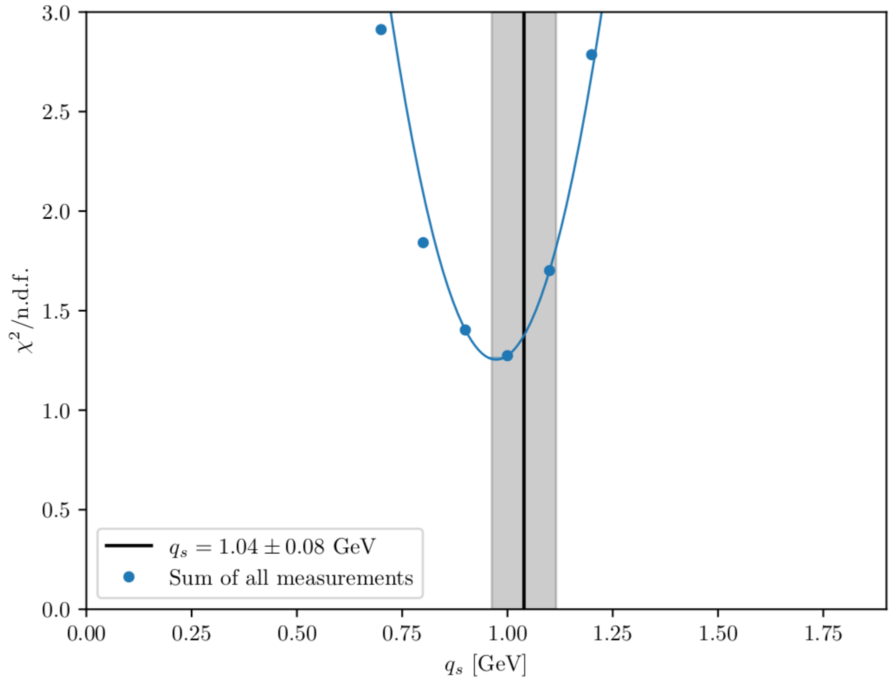

The global χ2 distribution exhibits a minimum at around q_s = 1.0 GeV, which is consistent with the value obtained from the measurement over a wide m_{DY} that includes a detailed uncertainty breakdown, with correlated experimental uncertainties.

Mass dependence of the intrinsic k_T

$M(l^+l^-)$ in DY events ~ hard scattering scale

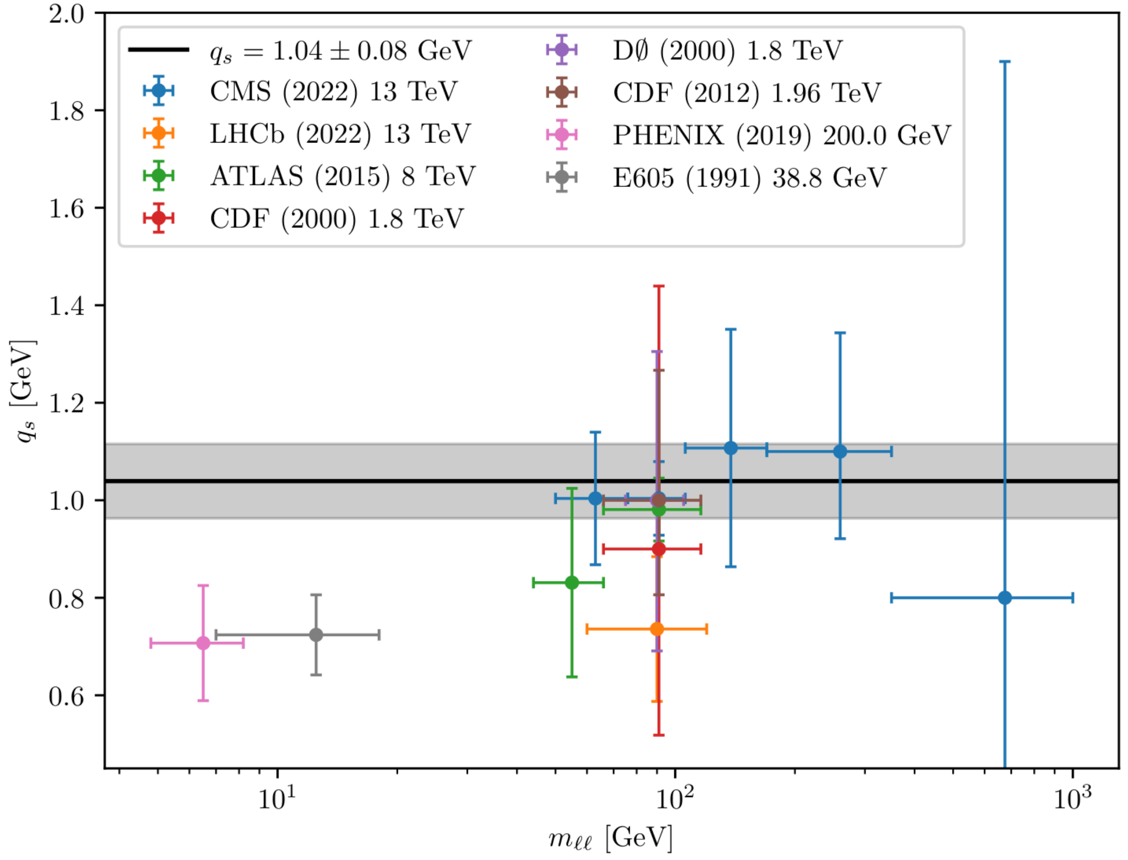

No dependence of q_s on various $m(l^+l^-)$ ranges

Energy dependence of the intrinsic k_T

Energy scaling behavior of intrinsic k_T width

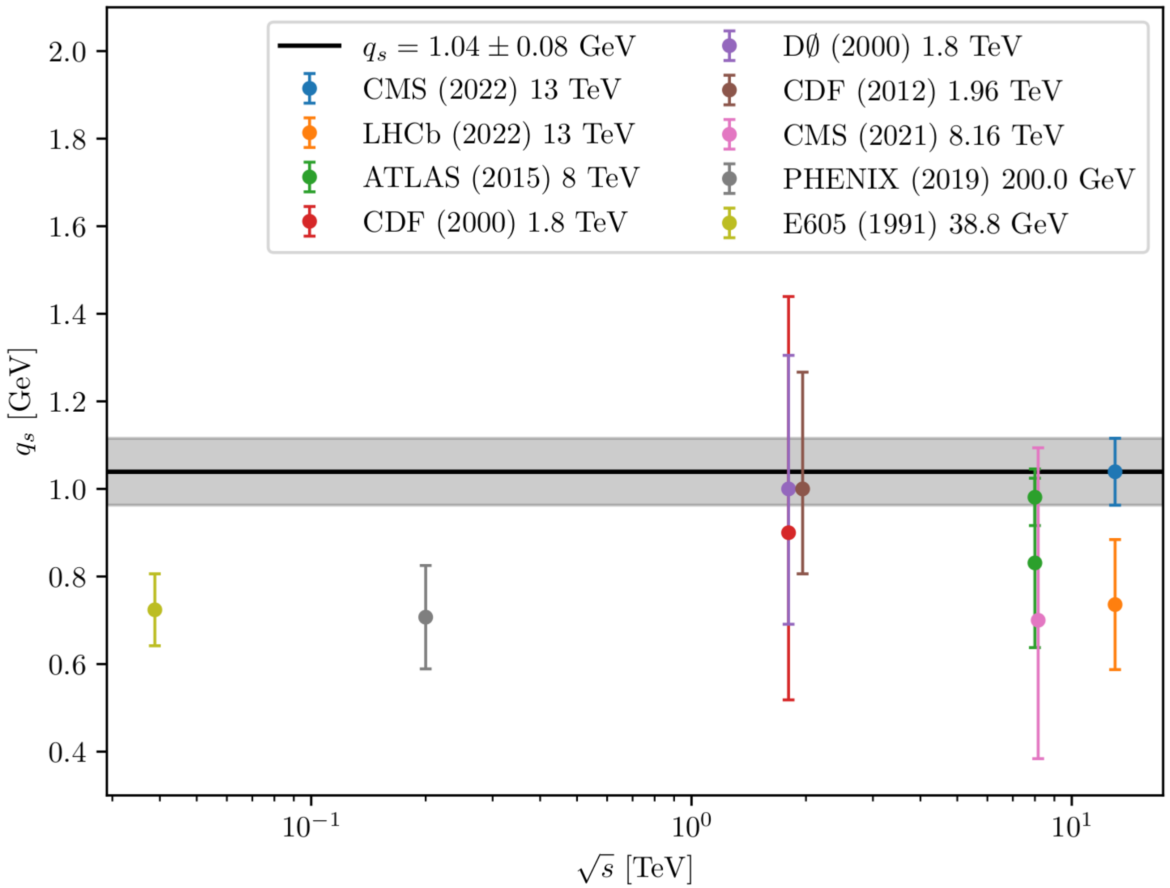

CASCADE: No/weak dependence of q_s on various center of mass energies from 32 GeV to 13TeV.

Conventional colinear MC generators: a Gaussian width exceeding the Fermi motion kinematics is needed to describe the measurements.

Summary and conclusions

Focus on Soft and Low Transverse Momenta in PB method: The treatment of most small k_T contributions in the PB method already handled within the Non-perturbative Sudakov form factor → only a small contribution of pure intrinsic k_T is needed.

Significance of Non-Perturbative sudakov form factor: The importance of the soft, non-perturbative region is demonstrated for both integrated and transverse momentum distributions.

Stability of Intrinsic-k_T Parameter: Our significant outcome is the extraction of the intrinsic-k_T parameter q_s from DY cross section, yielding a consistent value of q_s = 1.04 ± 0.08 GeV valid across various mass ranges (~10-1000 GeV) and center-of-mass energies (32 GeV to 13 TeV).

Contrast to Standard Monte Carlo Generators: Our results challenge the commonly used width values for intrinsic Gauss distributions in standard Monte Carlo event generators, which vary with center-of-mass energy.

Thank you for your attention !

BACK UP SLIDES

α_s scale

PB-Set1 (with DGLAP-type $\alpha_s(\mu^2)$) and PB-Set2 (with angular-ordered scale $\alpha_s(p_T^2=\mu^2(1-z)^2)$)

PB-Sets are fitted to precision DIS HERA measurements using the xFitter platform (χ^2/dof=1.21)
Accessible in TMDlib and TMDplotter
Both having q_s=0.5 GeV

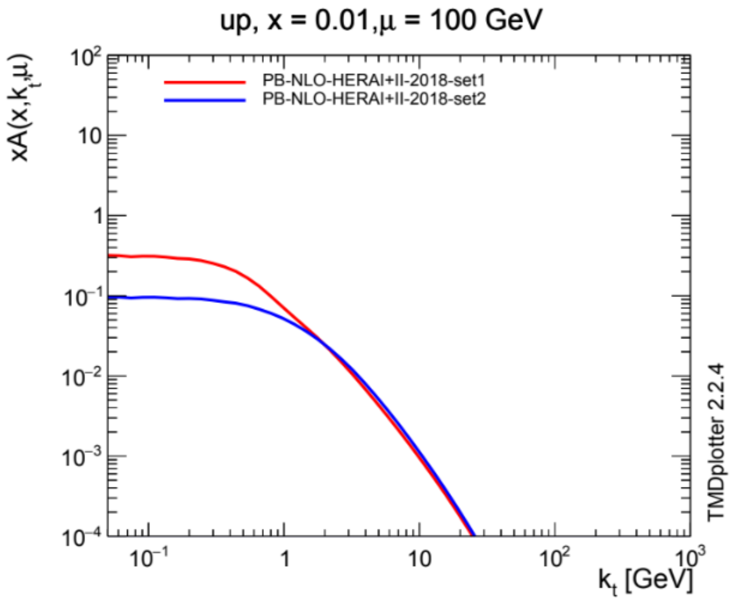

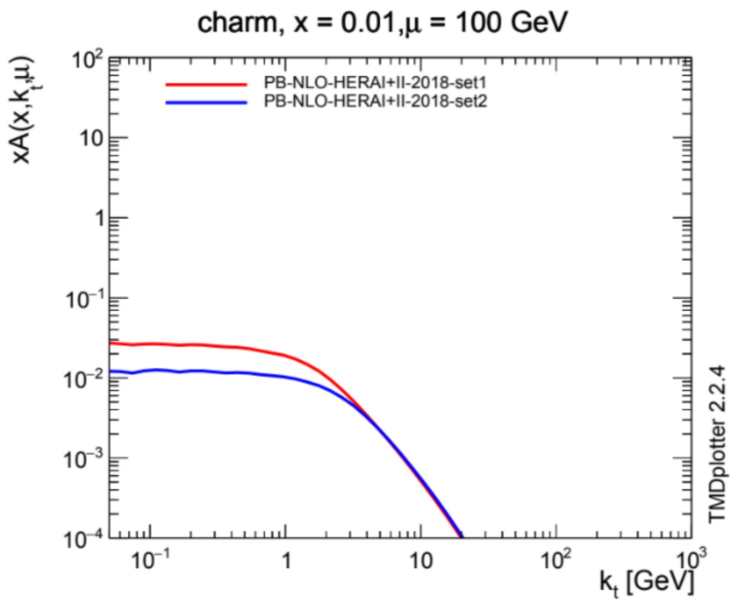

- Significant difference at low transverasal momenta of partons
- For heavy flavors the difference much smaller since they are only generated dynamically
- **PB-Set2** provides a much better description of measured Z/γ p_T at LHC, in low-energy experiments, and of di-jet Δφ near the back-to-back region. This underlines the relevance of the angular-ordered coupling in regions dominated by soft emissions.

Scale Dependence of Intrinsic k_T Sensitivity in TMD and DY p_T

Why lowest DY mass region is the most sensitive one?

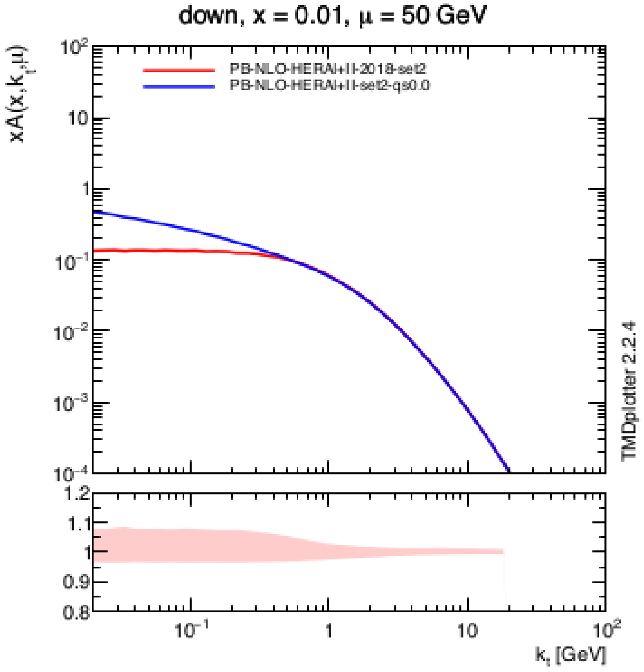

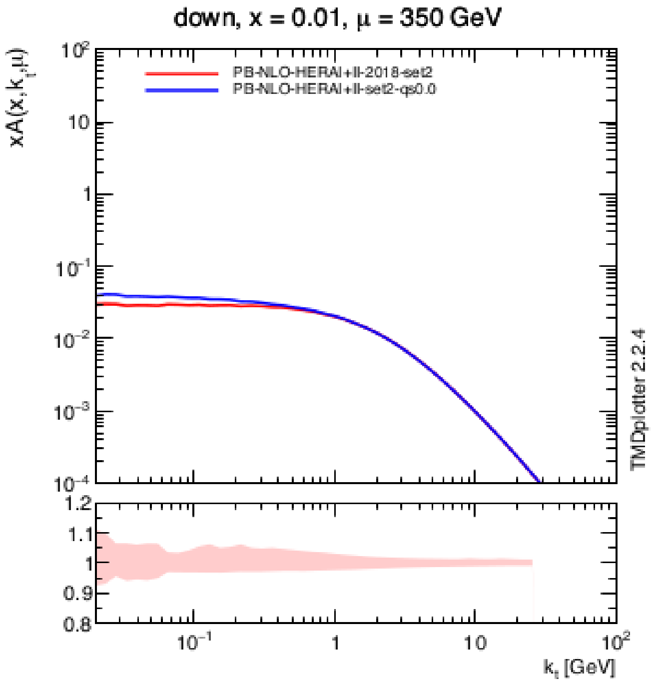

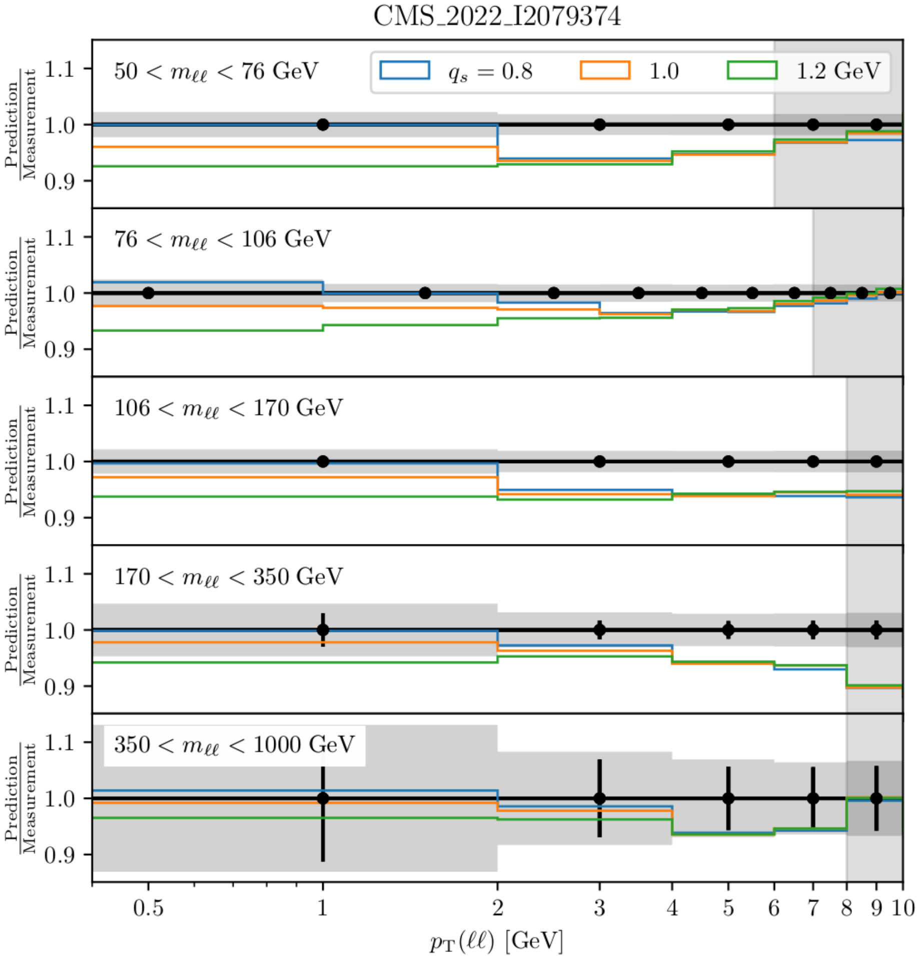

In TMD perspective: as the scale increases, sensitivity to intrinsic k_T decreases.

In DY p_T perspective: higher DY masses show reduced sensitivity to intrinsic k_T.